

Dynamic Modeling of Branched Robots using Modular Composition

Frederico Fernandes Afonso Silva and Bruno Vilhena Adorno

Abstract—This letter proposes a systematic modular procedure for the dynamic modeling of branched robots comprising several subsystems, each of which being composed of multiple rigid bodies. Furthermore, the proposed strategy is applicable even if some subsystems are regarded as black boxes, requiring only the twists and wrenches at the connection points between different subsystems. To help in the model composition, we also propose a graph representation that encodes the propagation of twists and wrenches between the subsystems. Numerical results show that the proposed formalism is as accurate as a state-of-the-art library for robotic dynamic modeling.

Index Terms—Modular dynamic modeling, Newton-Euler formalism, Topological graph.

I. INTRODUCTION

In robotics, the Newton-Euler formalism is usually presented at the level of each rigid body in the robotic structure, notably, the “ i -th link/joint/CoM.” This provides a systematic dynamic modeling strategy applicable to serial manipulators [1], [2] and open kinematic trees [3], [4], [5]. However, approaches based on this formalism typically give a monolithic solution to the system and do not allow model composition [6].

There are plenty of motivations for seeking a systematic dynamic model composition formalism. One could be assembling a robot using existing systems whose dynamic models are already known, such as the limbs of a humanoid robot. In a different scenario, a self-reconfiguring modular robot [7], [8], [9] could possess the dynamic information of its modules. From a control perspective, one could be interested in applying distributed control strategies to the subsystems comprising a complex dynamic structure.

A. Related works

Jain [10] proposed a technique of partitioning and aggregating graphs that allows the consideration of subsystems in the dynamic modeling of multibody systems. Subgraph elements are used to compose the mass matrix and the vector of nonlinear Coriolis and gyroscopic terms of the aggregated system, and then the stacked vector of generalized forces is calculated. Despite the system being composed of individual modules, full knowledge of the masses, inertia tensors, Coriolis accelerations, and gyroscopic terms of the whole system is required.

F. F. A. Silva is with the Graduate Program in Electrical Engineering, Federal University of Minas Gerais, Av. Antônio Carlos 6627, 31270-901, Belo Horizonte-MG, Brazil (email: fredf.afonso@gmail.com).

B. V. Adorno is with the Department of Electrical and Electronic Engineering, The University of Manchester, Sackville Street, Manchester M13 9PL, United Kingdom (email: bruno.adorno@manchester.ac.uk).

This work was supported by the Brazilian agency CAPES.

McPhee et al. [11] presented a strategy that uses individual subsystem models to derive the dynamic model of mechatronic multibody systems. Their approach uses free vectors and rotational matrices, thus decoupling translational and rotational components, which requires separate graphs. Moreover, that formalism relies on a symbolic implementation, and each subsystem must be symbolically derived before the modeling process for the complete system starts.

Moving away from graph representations, Orsino and Hess-Coelho [12] proposed a strategy for the modular modeling of multibody systems based on the dynamic invariant equations of its subsystems. Orsino [13] extended this formalism by proposing a hierarchical description of lumped-parameter dynamic systems that lead to a recursive modeling methodology. Albeit those formulations do not impose limitations on how the dynamic equations of each subsystem must be obtained, the final result is not given in terms of the generalized forces of the overall dynamic system but rather by its dynamic invariants. Thus, this strategy is not readily applicable to robotics problems where one typically needs to find the joint forces/torques as a function of the robot dynamics, which then are used to design suitable control laws.

More recently, Hess-Coelho et al. [14] presented a dynamic modular modeling methodology for parallel mechanisms. They use the hierarchical description proposed by Orsino [13] but follows a different approach to derive the model. Jacobian matrices of the subsystem’s angular and linear velocities are used with the Principle of Virtual Power to obtain the Euler-Lagrange model of the robot, and modularity is achieved by using a library of subsystem models. Nonetheless, the process of obtaining such models is highly dependent on geometric analysis of the system (i.e., inverse kinematics) and, if there is no library containing the subsystems’ models, the robot dynamics is found monolithically. Moreover, due to the free-vector representation, translational and rotational components are decoupled.

In conclusion, the existing model composition strategies oftentimes generate different graph representations for the translational and rotational components, increasing the overall complexity, and either require the previous construction of subsystem libraries or demand full knowledge of the dynamic elements of the whole system. Some of them also require a symbolic derivation, as opposed to recursive formulations, which makes it harder to model reconfigurable systems. This paper presents a systematic methodology that overcomes those drawbacks.

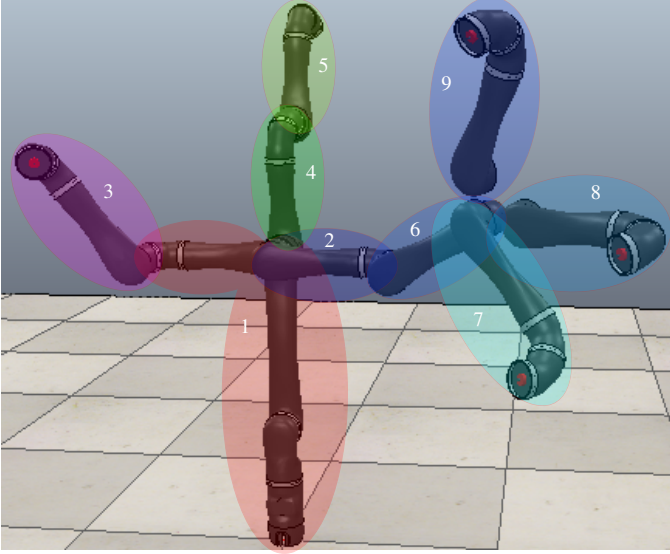


Figure 1: A 38-DoF branched robot composed of nine subsystems represented by the colored ellipses.

B. Statement of contributions

This paper presents the following contributions to the state-of-the-art:

- 1) A strategy for dynamic model composition, shown in Section II, that is applicable even if some subsystems are regarded as black boxes, requiring only the twists and wrenches at the connection points between different subsystems. Such information can be obtained either from previous calculations or sensor readings.
- 2) A unified graph representation of the system, shown in Section II-A, that provides the joint wrenches from the calculation of the graph interconnection matrix, in addition to visually depicting the model composition.
- 3) Finally, the proposed formulation imposes no restrictions regarding the algebra used to represent twists and wrenches, as long as some basic properties are respected. Nonetheless, we present an instantiation for dual quaternion algebra in Section III.

We perform a numerical evaluation of a fixed-base 38-DOF branched robot, and compare our results with the ones provided by a realistic simulator and with Featherstone's state-of-the-art library for robotic dynamic modeling [3].

II. MODEL COMPOSITION

Consider a branched robot such as the one shown in Fig. 1, which is composed of s subsystems. Given the interconnection points between pair of subsystems and the twists and wrenches applied at those points, our goal is to obtain a set of equations that describe the whole-body dynamics as a function of the dynamics of each subsystem $i \in \{1, \dots, s\} \triangleq S$.

Given the subsystem $i \in S$ that immediately precedes and is connected to $j \in \{j_{i,1}, \dots, j_{i,m_i}\} \triangleq S_i \subset S$, we assume that the first link of subsequent subsystems $j \in S_i$ can be connected to any link of the preceding subsystem i . For example, in Fig. 1, the first link of subsystem 3 is connected to the final

link of subsystem 1, whereas the first links of subsystems 2 and 4 are connected to the second link of subsystem 1.

Being the complete system an open kinematic tree, each subsystem can only be preceded by one subsystem but can be succeeded by several kinematic chains. Therefore, twists generated by the subsystem i will be propagated to each $j \in S_i$ and all other subsequent subsystems. On the other hand, the combined wrenches from all $j \in S_i$ will affect i and all its preceding subsystems.

Because the forward propagation of twists and the backward propagation of wrenches also happen within each subsystem, the idea is similar to the classic Newton-Euler algorithm [15]. Indeed, consider that each subsystem $i \in S$ is composed of n_i joints/links, is preceded by a subsystem $p_i \in S$, and is immediately succeeded by the subsystems $j \in S_i$. Also, consider a function $\mathcal{W}_i : \mathbb{T}^{2n_i} \rightarrow \mathbb{W}^{n_i}$ that maps the stacked vector $\underline{\Xi}_i \triangleq \begin{bmatrix} \underline{\Xi}_i^T & \dot{\underline{\Xi}}_i^T \end{bmatrix}^T \in \mathbb{T}^{2n_i}$ of total twists $\underline{\Xi}_i \in \mathbb{T}^{n_i}$ and twist time derivatives $\dot{\underline{\Xi}}_i \in \mathbb{T}^{n_i}$ at the center of mass (CoM) of each link in the i th subsystem to the corresponding vector of total wrenches $\underline{\Gamma}_i \in \mathbb{W}^{n_i}$ at the n_i joints.¹ The wrenches at the joints of each subsystem $i \in S$ originate from three sources: the twists and their time derivatives at the CoMs of each link in the i th subsystem; the twist and its time derivative at the connection point a_i with the preceding subsystem p_i ; and the wrenches at the connection points $b_{i,j}$ with each $j \in S_i$. Therefore,

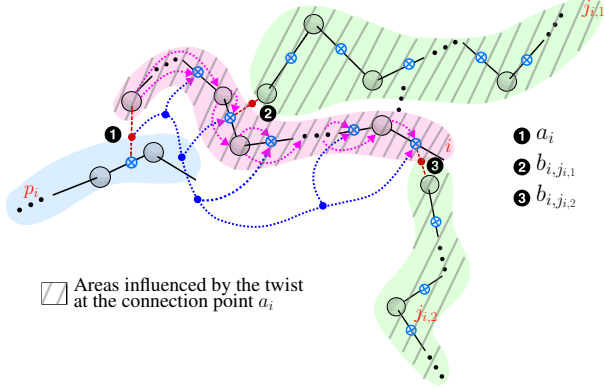
$$\underline{\Gamma}_i = \mathcal{W}_i(\underline{\Xi}_i) + \sum_{j \in S_i} \underline{\Gamma}_{j,i}, \quad \text{with } \underline{\Xi}_i = \underline{\Xi}_{p_i,i} + \underline{\Xi}_{i,i}, \quad (1)$$

where $\underline{\Xi}_{i,i} \triangleq \begin{bmatrix} \underline{\Xi}_{i,i}^T & \dot{\underline{\Xi}}_{i,i}^T \end{bmatrix}^T \in \mathbb{T}^{2n_i}$ is the stacked vector of twists and twist time derivatives at the n_i CoMs of subsystem $i \in S$; the elements of $\underline{\Xi}_{p_i,i} \triangleq \begin{bmatrix} \underline{\Xi}_{p_i,i}^T & \dot{\underline{\Xi}}_{p_i,i}^T \end{bmatrix}^T \in \mathbb{T}^{2n_i}$ are the twists and twist time derivatives at the connection point a_i expressed in each of the n_i CoMs of subsystem i ; and the elements of $\underline{\Gamma}_{j,i} \in \mathbb{W}^{n_i}$ are the wrenches of the connection point $b_{i,j}$ with $j \in S_i$ expressed in each of the $\eta \leq n_i$ joints of subsystem i that precedes $b_{i,j}$. More specifically, $\underline{\Gamma}_{j,i} = \begin{bmatrix} \underline{\Gamma}_{j,i}^T & \mathbf{0}_{n_i-\eta}^T \end{bmatrix}^T \in \mathbb{W}^{n_i}$ where $\underline{\Gamma}_{j,i} \in \mathbb{W}^\eta$ is the vector of wrenches at the η joints preceding the connection point² $b_{i,j}$, and $\mathbf{0}_{n_i-\eta} \in \mathbb{W}^{n_i-\eta}$ is a vector of zeros in the set \mathbb{W} . For example, if $\mathbb{W} = \mathbb{R}^6$, then $\mathbf{0}_{n_i-\eta} \in \mathbb{W}^{n_i-\eta}$ is equivalent to $\mathbf{0}_{6(n_i-\eta)} \in \mathbb{R}^{6(n_i-\eta)}$. If $\mathbb{W} = \mathcal{H}_p$, which is the set of pure dual quaternions [16], then $\mathbf{0}_{n_i-\eta} \in \mathbb{R}^{n_i-\eta}$ because $\mathcal{H}_p \ni 0 \in \mathbb{R}$ as $\mathbb{R} \subset \mathcal{H}_p$.

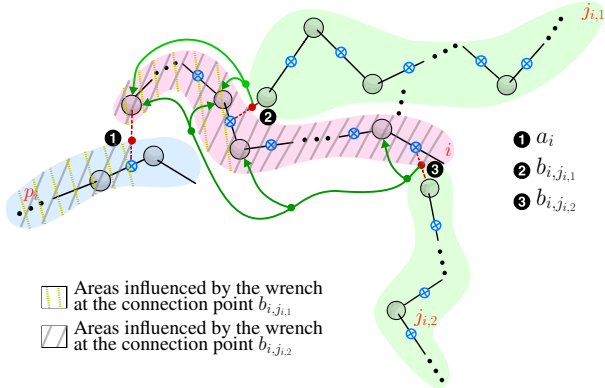
The wrenches generated at the joints of the i th subsystem as a result of its own motion, the motion of its predecessor, and the wrenches from its successors is shown in Fig. 2. The

¹The sets \mathbb{W} and \mathbb{T} of wrenches and twists, respectively, are six-dimensional manifolds that can be represented by different algebraic structures, such as six-dimensional vectors [3], four-by-four matrices [4], or pure dual quaternions [16].

²Joints after the connection point are not directly affected by wrenches from subsequent subsystems. Nonetheless, because those wrenches will affect the first η joints of the i th subsystem, the remaining $n_i - \eta$ links will be indirectly affected because the twists (and their derivatives) at the η joints arising from this interaction will be propagated to the remaining $n_i - \eta$ links.



(a) Forward propagation of twists from subsystem p_i to the remaining subsystems of the branched robot. Hatched regions indicate the areas influenced by the twist at the connection point a_i .



(b) Backward propagation of wrenches from subsystems $j \in S_i$ to the remaining subsystems of the branched robot. Hatched and crosshatched regions indicate the areas influenced by the wrenches at the connection points $b_{i,j}$.

Figure 2: Wrenches generated at the joints of the i th subsystem (pink region). For each subsystem, the large gray circles represent joints, solid black lines represent links, and blue crossed circles represent CoMs. Subsystem p_i is given in blue, subsystems $j \in S_i$ are colored in green, and red circles on the red dashed lines, numbered from 1 to 3, indicate the connection points. Dotted arrows represent the forward propagation of twists, whereas solid arrows represent the backward propagation of wrenches.

connection point between p_i and the i th subsystem, denoted by 1 in Fig. 2, contains the *resultant* twist generated by all moving joints from the connection point up to the root node. On the other hand, the connection points between subsequent kinematic chains connected to the i th subsystem, denoted by 2 and 3, contain the *resultant* wrenches generated by those systems and all their successors.

Therefore, to calculate the wrenches at the joints of the i th subsystem, we need the information of the twists (and their time derivatives) at its CoMs, the twist (and its time derivative) at the connection point with its predecessor, and the wrenches at the connection points with its successors. Thus, even if some subsystems are presented as black boxes, the joint wrenches of the overall system can still be obtained, as long as we have this information (e.g., through sensor readings).

Table I summarizes all the relevant variables used in the model composition.

Table I: Summary of variables and symbols.

Notation	Definition
s	Number of subsystems of the branched robot.
S	Set containing all subsystems of the branched robot.
$S_i \subset S$	Set of all subsystems that succeed the i th subsystem of the branched robot.
$i \in S$	The i th subsystem of the branched robot.
$j \in S_i$	Subsystem j , one of the successors of the i th subsystem.
$p_i \in S$	Subsystem p_i , the predecessor of the i th subsystem.
a_i	Connection point between subsystems p_i and i .
$b_{i,j}$	Connection point between subsystems i and $j \in S_i$.
$n_i \in \mathbb{N}$	Number of joints/links of the i th subsystem.
$\eta \leq n_i$	Number of joints in subsystem i that precede $b_{i,j}$.
\mathcal{W}_i	Function that maps the stacked vector of total twists and twist time derivatives at the CoM of each link in the i th subsystem to the corresponding vector of wrenches at the n_i joints.
$\Xi_{i,i} \in \mathbb{T}^{2n_i}$	The stacked vector of twists and twist time derivatives, generated by the i th subsystem, at the n_i CoMs of subsystem $i \in S$.
$\Xi_{p_i,i} \in \mathbb{T}^{2n_i}$	The stacked vector of twists and twist time derivatives expressed in each of the n_i CoMs of subsystem i , resulting from the twist at the connection point a_i .
$\Xi_i \in \mathbb{T}^{2n_i}$	The stacked vector of <i>total</i> twists and twist time derivatives at the n_i CoMs of subsystem $i \in S$ (i.e., $\Xi_i = \Xi_{i,i} + \Xi_{p_i,i}$).
$\bar{\Gamma}_{j,i} \in \mathbb{W}^\eta$	The vector of wrenches at the $\eta \leq n_i$ joints of subsystem i due to the wrench at the connection point $b_{i,j}$, with $j \in S_i$.
$\dot{\Gamma}_{j,i} \in \mathbb{W}^{n_i}$	Stacked vector of wrenches, $\dot{\Gamma}_{j,i} = \begin{bmatrix} \bar{\Gamma}_{j,i}^T & \mathbf{0}_{n_i - \eta}^T \end{bmatrix}^T \in \mathbb{W}^{n_i}$, that is used to propagate the wrench at the connection point $b_{i,j}$ to all joints of subsystem i .
$\Gamma_i \in \mathbb{W}^{n_i}$	The vector of <i>total</i> wrenches at the n_i joints of subsystem $i \in S$.
$\mathbf{0}_n \in \mathbb{W}^n$	An n -dimensional vector of zeros in the set \mathbb{W} .

Example 1. Considering only subsystems 1 and 2 in Fig. 1, and neglecting the remaining subsystems, the vectors $\Gamma_1 \in \mathbb{W}^{n_1}$ and $\Gamma_2 \in \mathbb{W}^{n_2}$, with $n_1 = 6$ and $n_2 = 4$, of wrenches at the joints of subsystems 1 and 2, respectively, are given by

$$\begin{aligned} \Gamma_1 &= \mathcal{W}_1(\Xi_1) + \dot{\Gamma}_{2,1}, \\ \Gamma_2 &= \mathcal{W}_2(\Xi_2), \end{aligned} \quad (2)$$

where $\Xi_1 = \Xi_{1,1}$ and $\Xi_2 = \Xi_{1,2} + \Xi_{2,2}$.

For subsystem 1, which is the first in the chain, the wrenches at the joints are generated by the twists and their time derivatives at the CoMs of its own links, and by the reaction wrenches generated by subsystem 2. On the other hand, for subsystem 2, which is the last in the chain if we disregard the other subsystems, the wrenches at the joints are generated by the twists and their time derivatives at the CoMs of its own links, in addition to the twist (and its derivative) that subsystem 1 contributes through the connection point.

A. Graph representation

We can consider each subsystem in a branched robot as a vertex in a graph, in which directed, weighted edges represent the propagation of wrenches and twists (and twist time derivatives). The advantage of such representation is that in addition to visually depicting the model composition, it provides the joint wrenches from the calculation of the graph

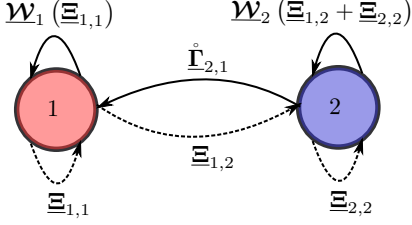


Figure 3: Graph representation of the 10-DoF assembled robot given by the first two subsystems shown in Fig. 1. The 6-DoF and the 4-DoF kinematic chains are labeled as systems 1 and 2, respectively.

interconnection matrix. For instance, the weighted graph in Fig. 3 represents the system of Example 1, where dashed edges correspond to the propagation of twists and their time derivatives, and solid edges represent the propagation of wrenches.

The interconnection matrix of the graph presented in Fig. 3 is given by

$$\underline{\mathbf{A}} = [\underline{\mathbf{A}}_{ij}] \triangleq \begin{bmatrix} \underline{\mathcal{W}}_1(\underline{\Xi}_1) & \underline{\Gamma}_{2,1} \\ \mathbf{0}_4 & \underline{\mathcal{W}}_2(\underline{\Xi}_2) \end{bmatrix} \in W^{10 \times 2}, \quad (3)$$

where $\underline{\Xi}_1 = \underline{\Xi}_{1,1}$ and $\underline{\Xi}_2 = \underline{\Xi}_{1,2} + \underline{\Xi}_{2,2}$. The vectors $\underline{\mathbf{A}}_{ij} \in W^{n_i}$ of the partitioned matrix $\underline{\mathbf{A}}$ indicates the propagation of wrenches from vertex j to vertex i , represented as a solid edge, in which n_i is the number of links of the i th subsystem. Because there is no wrench propagation from subsystem 1 to 2 in Example 1, $\underline{\mathbf{A}}_{2,1} = \mathbf{0}_4 \in W^4$, which is a vector of zeros in the set W . Therefore, since the corresponding "weight" is zero, there is no solid edge from 1 to 2 in the graph on Fig. 3. The interconnection matrix $\underline{\mathbf{A}}$ is analogous to the adjacency matrix of the graph. However, instead of simply indicating the existence of a connection between the vertices, the element $\underline{\mathbf{A}}_{ij}$ gives the joint wrenches imposed by one subsystem onto the other.

More generally, the graph representation of the complete system composed of s kinematic chains is constructed as follows:

- 1) Create a vertex for each kinematic chain.
- 2) Add the edges, according to the following rules:
 - a) Each vertex i has a dashed edge self-loop weighted by its own stacked vector of twists and twist time derivatives $\underline{\Xi}_{i,i} \in T^{2n_i}$;
 - b) Except for the vertex representing the root subsystem of the branched kinematic chain, each vertex i has an incoming dashed edge from the vertex p_i representing its predecessor, "weighted" by the stacked vector of twists and twist time derivatives $\underline{\Xi}_{p_i,i} \in T^{2n_i}$, and a solid edge self-loop weighted by its own vector of wrenches given by the $\underline{\mathcal{W}}_i(\underline{\Xi}_{i,i} + \underline{\Xi}_{p_i,i}) \in W^{n_i}$ function;
 - i) If the i th vertex represents the root subsystem of the branched kinematic chain, then the solid edge self-loop is weighted by $\underline{\mathcal{W}}_i(\underline{\Xi}_{i,i}) \in W^{n_i}$.
 - c) Except for the vertex representing the root subsystem of the branched kinematic chain, each vertex i has an outgoing solid edge that goes to the vertex p_i representing its predecessor, "weighted" by the vector of wrenches $\underline{\Gamma}_{i,p_i} \in W^{n_{p_i}}$.

Example 2. Consider the 38-DoF branched robot shown in Fig. 1, where $n_1 = 6$ and $n_2 = n_3 = \dots = n_9 = 4$. Following the procedure previously described, the weighted graph representing this robot is given in Fig. 4. Moreover, the interconnection matrix $\underline{\mathbf{A}} \in \mathcal{H}_p^{38 \times 9}$ is given by

$$\underline{\mathbf{A}} = \begin{bmatrix} \underline{\mathcal{W}}_1 & \underline{\Gamma}_{2,1} & \underline{\Gamma}_{3,1} & \underline{\Gamma}_{4,1} & \mathbf{0}_6 & \mathbf{0}_6 & \mathbf{0}_6 & \mathbf{0}_6 & \mathbf{0}_6 \\ \mathbf{0}_4 & \underline{\mathcal{W}}_2 & \mathbf{0}_4 & \mathbf{0}_4 & \mathbf{0}_4 & \underline{\Gamma}_{6,2} & \mathbf{0}_4 & \mathbf{0}_4 & \mathbf{0}_4 \\ \mathbf{0}_4 & \mathbf{0}_4 & \underline{\mathcal{W}}_3 & \mathbf{0}_4 & \mathbf{0}_4 & \mathbf{0}_4 & \mathbf{0}_4 & \mathbf{0}_4 & \mathbf{0}_4 \\ \mathbf{0}_4 & \mathbf{0}_4 & \mathbf{0}_4 & \underline{\mathcal{W}}_4 & \underline{\Gamma}_{5,4} & \mathbf{0}_4 & \mathbf{0}_4 & \mathbf{0}_4 & \mathbf{0}_4 \\ \mathbf{0}_4 & \mathbf{0}_4 & \mathbf{0}_4 & \mathbf{0}_4 & \underline{\mathcal{W}}_5 & \mathbf{0}_4 & \mathbf{0}_4 & \mathbf{0}_4 & \mathbf{0}_4 \\ \mathbf{0}_4 & \mathbf{0}_4 & \mathbf{0}_4 & \mathbf{0}_4 & \mathbf{0}_4 & \underline{\mathcal{W}}_6 & \underline{\Gamma}_{7,6} & \underline{\Gamma}_{8,6} & \underline{\Gamma}_{9,6} \\ \mathbf{0}_4 & \mathbf{0}_4 & \mathbf{0}_4 & \mathbf{0}_4 & \mathbf{0}_4 & \mathbf{0}_4 & \underline{\mathcal{W}}_7 & \mathbf{0}_4 & \mathbf{0}_4 \\ \mathbf{0}_4 & \underline{\mathcal{W}}_8 & \mathbf{0}_4 \\ \mathbf{0}_4 & \underline{\mathcal{W}}_9 \end{bmatrix},$$

where $\underline{\mathcal{W}}_i = \underline{\mathcal{W}}_i(\underline{\Xi}_{i,i})$ for $i = 1$ and $\underline{\mathcal{W}}_i = \underline{\mathcal{W}}_i(\underline{\Xi}_{p_i,i} + \underline{\Xi}_{i,i})$ for $i \in \{2, \dots, 9\}$, $p_2 = p_3 = p_4 = 1$, $p_5 = 4$, $p_6 = 2$, and $p_7 = p_8 = p_9 = 6$, and $\mathbf{0}_6 \in W^6$ and $\mathbf{0}_4 \in W^4$ are vectors of zeros in W^6 and W^4 , respectively.

The proposition below shows how the adjacency matrix is used to derive the model of the complete assembled system.

Proposition 3. Let a branched kinematic system be composed of n rigid bodies divided into a set of s coupled subsystems, each one containing n_1, n_2, \dots, n_s rigid bodies, respectively. Considering the proposed weighted graph representation with its corresponding adjacency matrix (3), the vector of joint wrenches $\underline{\Gamma}_{\text{total}}$ of the complete system is given by

$$\underline{\Gamma}_{\text{total}} = \begin{bmatrix} \underline{\Gamma}_1^T & \underline{\Gamma}_2^T & \dots & \underline{\Gamma}_s^T \end{bmatrix}^T = \underline{\mathbf{A}} \mathbf{1}_s \in W^n, \quad (4)$$

where $\underline{\Gamma}_i \in W^{n_i}$ is the vector of the total joint wrenches of the i th subsystem, $\underline{\mathbf{A}} \in W^{n \times s}$ is the interconnection matrix, with $n = \sum_{i=1}^s n_i$, and $\mathbf{1}_s \in W^s$ is an s -dimensional vector of identity elements (under the multiplication operation) in the set W .

Proof: Each element $\underline{\mathbf{A}}_{ij} \in W^{n_j}$ of the matrix $\underline{\mathbf{A}}$ represents the weight of the edge from vertex j to vertex i in the interconnection graph and, therefore, the propagation of wrenches from subsystem j to i . Hence, each row of $\underline{\mathbf{A}}$ contains all the wrenches acting upon the joints of the i th subsystem. Therefore, the vector $\underline{\Gamma}_i$ of the total joint wrenches of the i th subsystem is given by $\underline{\Gamma}_i = \sum_{j=1}^s \underline{\mathbf{A}}_{ij} = \sum_{j=1}^s \underline{\mathbf{A}}_{ij} \cdot \mathbf{1}$, where $\mathbf{1} \in W$ is the identity element³ in W under the multiplication operation. Thus, $\underline{\Gamma}_{\text{total}} = \underline{\mathbf{A}} \mathbf{1}_s$. ■

III. MODEL COMPOSITION USING DUAL QUATERNION ALGEBRA

The framework presented in Section II is general, has a high level of abstraction, and thus can be instantiated into different mathematical representations. Here we present one instance based on dual quaternion algebra,⁴ which is particularly suitable because elements such as unit dual quaternions and pure

³If $W = \mathbb{R}^6$ or $W = \mathcal{H}_p$ (i.e., a pure dual quaternion), then $\mathbf{1}_s = \mathbf{1}_s \in \mathbb{R}^s$. If $W \in \text{se}^*(3)$, then $\mathbf{1} = \mathbf{I}_{6 \times 6}$ and hence $\mathbf{1}_s \in \mathbb{R}^{(6 \sum_{i=1}^s n_i) \times 6}$.

⁴Basic definitions are shown in Appendix A. For a more comprehensive introduction of dual quaternion algebra, see [16].

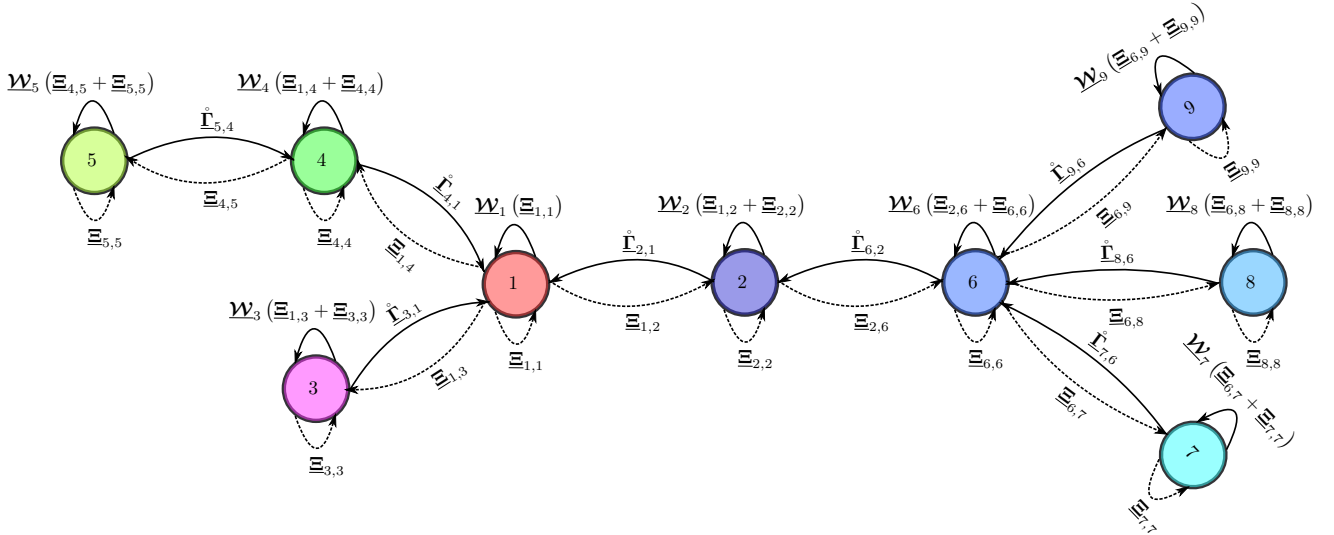


Figure 4: Graph representation of the 38-DoF branched robot. The colored nodes follow the color scheme adopted in Fig. 1. Only the root subsystem, represented by vertex 1, has just one incoming dashed edge, meaning that no twists are propagated from other subsystems. On the other hand, only the vertices corresponding to the leaves of the branched system (3, 5, 7, 8, and 9) have only one incoming solid edge, meaning that no wrenches are propagated from other subsystems.

dual quaternions, when equipped with standard multiplication and addition operations, form Lie groups with associated Lie algebras [17]. Furthermore, dual quaternion algebra provides an elegant and efficient representation of homogeneous transformations [18] and screw theory [19]. Nonetheless, other representations, such as the spatial algebra [3] or the Lie algebra se(3) [4], might also be used, as long as they capture the high-level operations described in Section II.

Consider the expressions in Section II. If dual quaternions are used, then $\mathcal{M} = \mathcal{T} = \mathcal{H}_p$, where \mathcal{H}_p is the set of pure dual quaternions; that is, dual quaternions with real part equal to zero (see Appendix A). Also, $\mathbf{1}_n = \mathbf{1}_n \in \mathbb{R}^n$ and $\mathbf{0}_n \in \mathbb{R}^n$ because $0, 1 \in \mathbb{R} \subset \mathcal{H}$, and $0\mathbf{x} = \mathbf{x}0 = 0$ and $1\mathbf{x} = \mathbf{x}1 = \mathbf{x}$ for any $\mathbf{x} \in \mathcal{H}$. Therefore, the high-level expressions used to propagate twists and wrenches remain unchanged, but the low-level expressions used to express those twists and wrenches in different frames must explicitly employ the operations of dual quaternion algebra.

More specifically, the twist $\xi_{0,a_i}^{a_i} \in \mathcal{H}_p$ at the connection point a_i between the preceding subsystem p_i and current subsystem i , propagated to each of the CoMs of subsystem i , is given by the vector of twists $\bar{\Xi}_{p_i,i} \in \mathcal{H}_p^{n_i}$ such that

$$\bar{\Xi}_{p_i,i} = \text{Ad}_{n_i}(\mathbf{X}_{p_i,i}) \xi_{0,a_i}^{a_i}, \quad (5)$$

where the (vector) adjoint operator Ad_{n_i} is given by (9) and $\mathbf{X}_{p_i,i} = [\mathbf{x}_{a_i}^{c_1} \ \dots \ \mathbf{x}_{a_i}^{c_{n_i}}]^T \in \mathcal{S}^{n_i}$ is the vector of the relative poses (i.e., unit dual quaternions) between the connection point a_i and the n_i CoMs of the i th subsystem. The vector of dual quaternions $\bar{\Xi}_{p_i,i} \in \mathcal{H}_p^{n_i}$ is given by the time derivative of (5), where each element is given by [20]

$$\begin{aligned} \frac{d}{dt} \left(\text{Ad}(\mathbf{x}_{a_i}^{c_k}) \xi_{0,a_i}^{a_i} \right) &= \text{Ad}(\mathbf{x}_{a_i}^{c_k}) \dot{\xi}_{0,a_i}^{a_i} \\ &+ \xi_{c_k,a_i}^{c_k} \times \left(\text{Ad}(\mathbf{x}_{a_i}^{c_k}) \xi_{0,a_i}^{a_i} \right), \quad (6) \end{aligned}$$

for $k \in \{1, \dots, n_i\}$.

Analogously, the wrench $\zeta_{0,b_{i,j}}^{b_{i,j}} \in \mathcal{H}_p$ at the connection point $b_{i,j}$ between the current subsystem i and the succeeding subsystem j , propagated to each of the CoMs of subsystem i , is given by the vector of wrenches $\bar{\Gamma}_{j,i} \in \mathcal{H}_p^{n_i}$ such that⁵

$$\bar{\Gamma}_{j,i} = \text{Ad}_{n_i}(\mathbf{X}_{j,i}) \zeta_{0,b_{i,j}}^{b_{i,j}}, \quad (7)$$

in which $\mathbf{X}_{j,i} = [\bar{\mathbf{X}}_{j,i}^T \ \mathbf{0}_{n_i-n}^T]^T \in \mathcal{S}^{n_i}$, with $\bar{\mathbf{X}}_{j,i} = [\mathbf{x}_{b_{i,j}}^0 \ \dots \ \mathbf{x}_{b_{i,j}}^\eta]^T \in \mathcal{S}^\eta$ being the vector of relative poses (i.e., unit dual quaternions) between the connection point $b_{i,j}$ and each of the $\eta \leq n_i$ joints of subsystem i that precede $b_{i,j}$.

The following example illustrates the application of the proposed modular composition strategy to derive the dynamic model of the subsystems 1 and 2 shown in Fig. 1.

Example 4. Consider the Example 1. If dual quaternions are used, then $\mathcal{W}^6 = \mathcal{H}_p^6$ and $\mathcal{W}^4 = \mathcal{H}_p^4$. Also, $\bar{\Gamma}_{2,1} = \text{Ad}_6(\mathbf{X}_{2,1}) \zeta_{0,b_{1,2}}^{b_{1,2}}$, where $\zeta_{0,b_{1,2}}^{b_{1,2}}$ is the wrench propagated from subsystem 2 to subsystem 1 at the connection point $b_{1,2} = a_2$, in which $\mathbf{X}_{2,1} = [\bar{\mathbf{X}}_{2,1}^T \ \mathbf{0}_4^T]^T \in \mathcal{S}^6$ and $\bar{\mathbf{X}}_{2,1} = [\mathbf{x}_{b_{1,2}}^0 \ \mathbf{x}_{b_{1,2}}^1]^T \in \mathcal{S}^2$. Only the first two elements of $\mathbf{X}_{2,1}$ are different from zero because the connection point $b_{1,2}$ is done at the final extremity of the second link of subsystem 1. Therefore, $\zeta_{0,b_{1,2}}^{b_{1,2}}$ does not directly affect the last four links. Moreover, $\bar{\Xi}_{1,2} = \text{Ad}_4(\mathbf{X}_{1,2}) \xi_{0,a_2}^{a_2}$, in which $\xi_{0,a_2}^{a_2}$ is the twist propagated from subsystem 1 to subsystem 2 at the connection point a_2 , and $\mathbf{X}_{1,2} = [\mathbf{x}_{a_2}^{c_1} \ \dots \ \mathbf{x}_{a_2}^{c_4}]^T \in \mathcal{S}^4$, where the symbol “ \cdot ” indicates the frames \mathcal{F}_{c_i} located at the

⁵It is important to notice that $\xi_{0,a_i}^{a_i}$ in (5) is the twist at connection point a_i with respect to frame \mathcal{F}_0 , expressed in frame \mathcal{F}_{a_i} . Analogously, $\zeta_{0,b_{i,j}}^{b_{i,j}}$ is the wrench at connection point $b_{i,j}$ with respect to frame \mathcal{F}_0 , expressed in frame $\mathcal{F}_{b_{i,j}}$.

CoM of each link in subsystem 2 (as opposed to the frames \mathcal{F}_{c_i} located at the CoM of each link in subsystem 1). Lastly, $\underline{\Xi}_{2,2} = \begin{bmatrix} \underline{\xi}_{0,\tilde{c}_1}^{\tilde{c}_1} & \cdots & \underline{\xi}_{0,\tilde{c}_4}^{\tilde{c}_4} \end{bmatrix}$ is the vector of twists at the CoMs of subsystem 2 that are caused exclusively by the motion of the joints of subsystem 2.

IV. NUMERICAL EVALUATION

To evaluate the accuracy of the methodology of model composition proposed in Sections II and III, we performed numerical evaluations using the 38-DoF branched robot shown in Fig. 1. We also compared it with the recursive Newton-Euler algorithm (sv2NE) available in Featherstone’s Spatial v2 package,⁶ which implements the robot dynamic modeling based on spatial algebra [3].

Spatial algebra has been used on actual complex robotic platforms, such as humanoids, thanks to its good accuracy and computational performance [21]. Therefore, it is a good basis of comparison. Nonetheless, we evaluated both our model and the Spatial v2 on the robot simulator V-REP PRO EDU V3.6.2 [22] with the Vortex Studio Academic physics engine⁷ as it offers high-fidelity results. The implementation was done in Matlab 2020a, and the computational library DQ Robotics [17] was used for dual quaternion algebra on a computer running Ubuntu 18.04 LTS 64 bits equipped with a Intel Core i7 6500U with 8GB RAM.

The robot followed a sinusoidal joint velocity trajectories given by $\dot{\mathbf{q}}_d = \sin(2\pi t) \mathbf{1}_{38} \text{ rad/s}$ using V-REP’s standard low-level controllers, and its joint configurations $\mathbf{q} \in \mathbb{R}^{38}$, joint velocities $\dot{\mathbf{q}} \in \mathbb{R}^{38}$, and joint torques $\boldsymbol{\tau} \in \mathbb{R}^{38}$ were read from V-REP and stored. Since the simulator does not allow the direct reading of accelerations, $\dot{\mathbf{q}}$ was filtered with a 6th-order discrete low-pass Butterworth filter with normalized cutoff frequency of 10Hz and used to obtain the joint accelerations $\ddot{\mathbf{q}} \in \mathbb{R}^{38}$ by means of numerical differentiation based on Richardson extrapolation [23, p. 322].

Using the values of \mathbf{q} , $\dot{\mathbf{q}}$, and $\ddot{\mathbf{q}}$, the twists at the CoMs of the branched robot were calculated [20] and used to obtain the joint wrenches $\underline{\Gamma}_{\text{dqNEMC}} \in \mathcal{H}_p^{38}$ through (1). Then, the wrenches were projected onto the joints motion axes yielding $\boldsymbol{\tau}_{\text{dqNEMC}} \in \mathbb{R}^{38}$ [20]. The comparisons between the joint torque waveforms $\boldsymbol{\tau}_{\text{dqNEMC}}$ and $\boldsymbol{\tau}$ were made considering the *coefficient of multiple correlation (CMC)* [24] between the waveforms. The CMC provides a coefficient ranging between zero and one that indicates how similar two given waveforms are. Identical waveforms have CMC equal to one, whereas completely different waveforms have CMC equal to zero. Moreover, the joint torques $\boldsymbol{\tau}_{\text{sv2NE}} \in \mathbb{R}^{38}$ were obtained from the sv2NE and the CMCs between them and the measured joint torques $\boldsymbol{\tau}$ were also calculated.

Table II presents the CMC between the joint torque waveforms obtained through the different dynamic model strategies (dqNEMC and sv2NE) and the values obtained from V-REP+Vortex. Both of them presented mean (mean) and minimum (min) CMC close to one, with small standard deviation

Table II: CMC between the joint torque waveforms obtained through different dynamic model strategies and the values obtained from V-REP. The closer to one, the more similar the waveforms are.

38-DoF branched robot				
Method	min	max	mean	std
dqNEMC	0.9850	1.0000	0.9968	0.0037
sv2NE	0.9850	1.0000	0.9968	0.0037

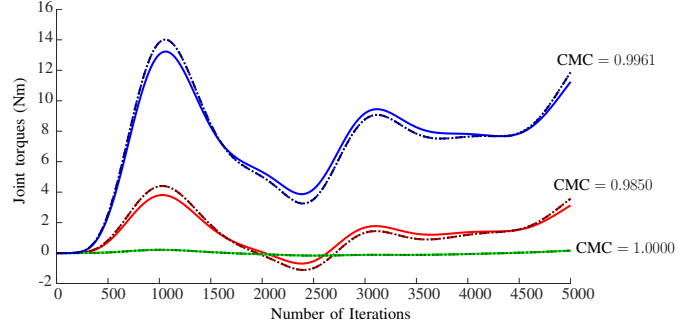


Figure 5: Three joint torque waveforms of the 38-DoF branched robot. *Solid* curves correspond to the V-REP values, whereas *dashed* curves correspond to the values obtained using the dqNEMC and *dot-dashed* curves correspond to the values obtained using the sv2NE for the joint torque waveforms of the eleventh (CMC = 0.9850), sixth (CMC = 1.0000), and third (CMC = 0.9961) joints, respectively. Because dqNEMC and sv2NE return the same results, their curves are superimposed.

(std) and high maximum (max) CMC, thus indicating high similarity between the joint torque waveform obtained from dqNEMC, sv2NE, and the values from V-REP.

Furthermore, the dqNEMC is numerically equivalent to the sv2NE, which demonstrates the accuracy of our proposed strategy when compared to Featherstone’s spatial recursive Newton-Euler algorithm. However, it is worth highlighting that the dqNEMC performs the modular dynamic modeling of the robot, whereas the sv2NE obtains the joint torques through a monolithic solution (i.e., without considering the existence of subsystems).

For qualitative analysis, Fig. 5 presents the joint torques obtained using dqNEMC and sv2NE, alongside the V-REP values, for the minimum, maximum, and intermediate CMCs found during simulations. Even for the smallest value of CMC (i.e., 0.9850), the joint torques obtained using our model composition formulation match closely the V-REP values. The small discrepancies arise from both discretization effects and uncertainties in the kinematic model.

V. CONCLUSIONS

This work presented a modular composition strategy for the dynamic modeling of branched robots. The proposed formalism requires only the twists, twist time derivatives, and wrenches at the connection points between different subsystems. Thus, the strategy works even when subsystems are black boxes, as long as the required information at the connection points are obtained through sensor readings. Furthermore, we also proposed a graph representation for the complete branched mechanism, in which each vertex is a serial kinematic chain, and the wrenches at the joints result from the graph interconnection matrix.

⁶Available at: <http://royfeatherstone.org/spatial/v2/>

⁷Available at: <https://www.cm-labs.com/vortex-studio/>

Simulation results have shown that our proposed strategy is numerically equivalent to monolithic solutions, such as Featherstone's Spatial $v2$ Newton-Euler algorithm, where the dynamic model is built considering the whole open kinematic tree at once.

Future works will focus on extending the proposed formulation to closed kinematic chains, and exploiting parallelization techniques for real-time calculation of the dynamic model of complex branched robots with a very large number of degrees of freedom.

APPENDIX A DUAL QUATERNION ALGEBRA

Dual quaternions [5] are elements of the set

$$\mathcal{H} \triangleq \{\mathbf{h}_P + \varepsilon \mathbf{h}_D : \mathbf{h}_P, \mathbf{h}_D \in \mathbb{H}, \varepsilon \neq 0, \varepsilon^2 = 0\},$$

where $\mathbb{H} \triangleq \{h_1 + \hat{i}h_2 + \hat{j}h_3 + \hat{k}h_4 : h_1, h_2, h_3, h_4 \in \mathbb{R}\}$ is the set of quaternions, in which \hat{i} , \hat{j} and \hat{k} are imaginary units with the properties $\hat{i}^2 = \hat{j}^2 = \hat{k}^2 = \hat{i}\hat{j}\hat{k} = -1$ [5]. Addition and multiplication of dual quaternions are analogous to their counterparts of real and complex numbers. One must only respect the properties of the dual unit ε and imaginary units \hat{i} , \hat{j} , \hat{k} .

The subset $\underline{\mathcal{S}} = \{\mathbf{h} \in \mathcal{H} : \|\mathbf{h}\| = 1\}$ of unit dual quaternions, where $\|\mathbf{h}\| = \sqrt{\mathbf{h}\mathbf{h}^*} = \sqrt{\mathbf{h}^*\mathbf{h}}$, with \mathbf{h}^* being the conjugate of \mathbf{h} [16], is used to represent poses (position and orientation) in the three-dimensional space and form the group $\text{Spin}(3) \times \mathbb{R}^3$ under the multiplication operation. Any $\mathbf{x} \in \underline{\mathcal{S}}$ can always be written as $\mathbf{x} = \mathbf{r} + \varepsilon(1/2)\mathbf{p}\mathbf{r}$, where $\mathbf{p} = \hat{i}x + \hat{j}y + \hat{k}z$ represents the position (x, y, z) in the three-dimensional space and $\mathbf{r} = \cos(\phi/2) + \mathbf{n}\sin(\phi/2)$ represents a rotation, in which $\phi \in [0, 2\pi)$ is the rotation angle around the rotation axis $\mathbf{n} \in \mathbb{H}_p \cap \mathbb{S}^3$, with $\mathbb{H}_p \triangleq \{\mathbf{h} \in \mathbb{H} : \text{Re}(\mathbf{h}) = 0\}$, where $\text{Re}(h_1 + \hat{i}h_2 + \hat{j}h_3 + \hat{k}h_4) \triangleq h_1$, and $\mathbb{S}^3 = \{\mathbf{h} \in \mathbb{H} : \|\mathbf{h}\| = 1\}$ [5].

The set $\mathcal{H}_p = \{\mathbf{h} \in \mathcal{H} : \text{Re}(\mathbf{h}) = 0\}$ of pure dual quaternions is used to represent twists and wrenches, which are represented in different coordinate systems using the adjoint operator $\text{Ad} : \underline{\mathcal{S}} \times \mathcal{H}_p \rightarrow \mathcal{H}_p$. For instance, consider the twist $\underline{\xi}^a \in \mathcal{H}_p$ expressed in frame \mathcal{F}_a and the unit dual quaternion \underline{x}_a^b that represents the rigid motion from \mathcal{F}_b to \mathcal{F}_a . The same twist is expressed in frame \mathcal{F}_b as

$$\underline{\xi}^b = \text{Ad}(\underline{x}_a^b)\underline{\xi}^a = \underline{x}_a^b \underline{\xi}^a (\underline{x}_a^b)^*. \quad (8)$$

The next definition extends the adjoint operation (8) to the set \mathcal{H}_p^n .

Definition 5. Given a vector of poses $\underline{\mathbf{X}} = [\underline{x}_1 \ \underline{x}_2 \ \cdots \ \underline{x}_n]^T \in \underline{\mathcal{S}}^n$ and a pure dual quaternion $\underline{\mathbf{a}} \in \mathcal{H}_p$, the operator $\text{Ad}_n : \underline{\mathcal{S}}^n \times \mathcal{H}_p \rightarrow \mathcal{H}_p^n$ is defined as

$$\begin{aligned} \text{Ad}_n(\underline{\mathbf{X}})\underline{\mathbf{a}} &\triangleq \text{diag}(\underline{\mathbf{X}})\underline{\mathbf{a}}\underline{\mathbf{X}}^{*T} \\ &= [\text{Ad}(\underline{x}_1)\underline{\mathbf{a}} \ \text{Ad}(\underline{x}_2)\underline{\mathbf{a}} \ \cdots \ \text{Ad}(\underline{x}_n)\underline{\mathbf{a}}]^T \end{aligned} \quad (9)$$

where $\text{diag}(\underline{\mathbf{X}}) \in \mathcal{H}_p^{n \times n}$ is a diagonal matrix with the elements of $\underline{\mathbf{X}}$ in the main diagonal, and $\underline{\mathbf{X}}^*$ is the conjugate transpose of $\underline{\mathbf{X}}$.

REFERENCES

- [1] B. Siciliano, L. Sciavicco, L. Villani, and G. Oriolo, *Robotics*, ser. Advanced Textbooks in Control and Signal Processing. London: Springer London, 2009.
- [2] M. W. Spong, S. Hutchinson, and M. Vidyasagar, *Robot Modeling and Control*. New York: Wiley, 2006.
- [3] R. Featherstone, *Rigid body dynamics algorithms*. Springer, 2008.
- [4] R. M. Murray, Z. Li, and S. S. Sastry, *A Mathematical Introduction to Robotic Manipulation*, 1st ed. CRC Press, 1994.
- [5] J. M. Selig, *Geometric Fundamentals of Robotics*, 2nd ed., ser. Monographs in Computer Science. New York, NY: Springer New York, 2005.
- [6] B. Siciliano and O. Khatib, *Springer Handbook of Robotics*, B. Siciliano and O. Khatib, Eds. Berlin, Heidelberg: Springer Berlin Heidelberg, 2008.
- [7] K. Kotay, D. Rus, M. Vona, and C. McGray, "The self-reconfiguring robotic molecule," in *Proceedings. 1998 IEEE Int. Conf. Robot. Autom. (Cat. No.98CH36146)*, vol. 1, no. May. IEEE, 1998, pp. 424–431. [Online]. Available: <http://ieeexplore.ieee.org/document/676452/>
- [8] J. Neubert and H. Lipson, "Soldercubes: a self-soldering self-reconfiguring modular robot system," *Auton. Robots*, vol. 40, no. 1, pp. 139–158, jan 2016. [Online]. Available: <http://link.springer.com/10.1007/s10514-015-9441-4>
- [9] C. Unsal and P. Khosla, "Mechatronic design of a modular self-reconfiguring robotic system," in *Proc. 2000 ICRA. Millenn. Conf. IEEE Int. Conf. Robot. Autom. Symp. Proc.*, vol. 2. IEEE, 2000, pp. 1742–1747. [Online]. Available: <https://doi.org/10.1109/ROBOT.2000.844847>
- [10] A. Jain, "Multibody graph transformations and analysis," *Nonlinear Dyn.*, vol. 67, no. 4, pp. 2779–2797, mar 2012. [Online]. Available: <http://link.springer.com/10.1007/s11071-011-0188-y>
- [11] J. McPhee, C. Schmitke, and S. Redmond, "Dynamic Modelling of Mechatronic Multibody Systems With Symbolic Computing and Linear Graph Theory," *Math. Comput. Model. Dyn. Syst.*, vol. 10, no. 1, pp. 1–23, mar 2004. [Online]. Available: <https://doi.org/10.1080/13873950412331318044>
- [12] R. M. Matarazzo Orsino and T. A. Hess-Coelho, "A contribution to the modular modelling of multibody systems," *Proc. R. Soc. A Math. Phys. Eng. Sci.*, vol. 471, no. 2183, p. 20150080, nov 2015.
- [13] R. M. M. Orsino, "Recursive modular modelling methodology for lumped-parameter dynamic systems," *Proc. R. Soc. A Math. Phys. Eng. Sci.*, vol. 473, no. 2204, p. 20160891, 2017.
- [14] T. A. Hess-Coelho, R. M. M. Orsino, and F. Malvezzi, "Modular modelling methodology applied to the dynamic analysis of parallel mechanisms," *Mech. Mach. Theory*, vol. 161, p. 104332, jul 2021.
- [15] J. Y. S. Luh, M. W. Walker, and R. P. C. Paul, "On-Line Computational Scheme for Mechanical Manipulators," *J. Dyn. Syst. Meas. Control*, vol. 102, no. 2, pp. 69–76, jun 1980.
- [16] B. V. Adorno, "Robot Kinematic Modeling and Control Based on Dual Quaternion Algebra – Part I: Fundamentals," 2017. [Online]. Available: <https://hal.archives-ouvertes.fr/hal-01478225v1>
- [17] B. V. Adorno and M. Marques Marinho, "DQ Robotics: A Library for Robot Modeling and Control," *IEEE Robot. Autom. Mag.*, vol. 28, no. 3, pp. 102–116, sep 2021. [Online]. Available: <https://ieeexplore.ieee.org/document/9136790/>
- [18] J. Funda, R. H. Taylor, and R. P. Paul, "On Homogeneous Transforms, Quaternions, and Computational Efficiency," *IEEE Trans. Robot. Autom.*, vol. 6, no. 3, pp. 382–388, 1990.
- [19] N. A. Aspragathos and J. K. Dimitros, "A comparative study of three methods for robot kinematics," *IEEE Trans. Syst. Man, Cybern. Part B Cybern.*, vol. 28, no. 2, pp. 135–145, 1998.
- [20] F. F. A. Silva, J. J. Quiroz-Omaña, and B. V. Adorno, "Dynamics of Mobile Manipulators using Dual Quaternion Algebra," *J. Mech. Robot.*, pp. 1–24, apr 2022. [Online]. Available: <https://arxiv.org/abs/2007.08444>
- [21] K. Bouyarmane, K. Chappellet, J. Vaillant, and A. Kheddar, "Quadratic Programming for Multirobot and Task-Space Force Control," *IEEE Trans. Robot.*, vol. 35, no. 1, pp. 64–77, feb 2019.
- [22] E. Rohmer, S. P. N. Singh, and M. Freese, "V-REP: A versatile and scalable robot simulation framework," in *22013 IEEE/RSJ Int. Conf. Intell. Robot. Syst.* IEEE, nov 2013, pp. 1321–1326.
- [23] A. Gilat and V. Subramaniam, *Numerical Methods for Engineers and Scientists: An Introduction with Applications using MATLAB*, 3rd ed., L. Ratts and H. Ellis, Eds. Hoboken, USA: John Wiley & Sons, 2014.
- [24] A. Ferrari, A. G. Cutti, and A. Cappello, "A new formulation of the coefficient of multiple correlation to assess the similarity of waveforms measured synchronously by different motion analysis protocols," *Gait & Posture*, vol. 31, no. 4, pp. 540–542, apr 2010.